HIGHER DIMENSIONAL FLEXURE MODE FOR ENHANCED EFFECTIVE ELECTROMECHANICAL COUPLING IN PZT-ON-SILICON MEMS RESONATORS

J.M. Puder[1,2], S.S. Bedair[2], J.S. Pulskamp[2], R.Q. Rudy[2], R.G. Polcawich[2], and S.A. Bhave[1]
[1]Oxide MEMS Group, Cornell University, Ithaca, NY, USA
[2]Piezo MEMS Group, Army Research Laboratory, MD, USA

ABSTRACT

This paper reports on a low-loss, flexural-mode resonator with enhanced effective electromechanical coupling, k_{eff}^2. Improvement is achieved by utilizing a higher dimensional vibrational mode that possesses more than one non-zero, in-phase normal-stress component. Specifically, the stress profile augments coupling with contributions from both the d_{31} and d_{32} piezoelectric coefficients. The 52.6 MHz flexure-based mode of the 0.5-µm lead zirconate titanate (PZT) on 4-µm silicon resonator yields ~4x boost in k_{eff}^2 (2.07% versus 0.55%) when compared with the fundamental length-extensional mode of the same device. Measurements also reveal a 50 Ω terminated insertion loss (IL) of -3.6 dB and motional resistance, R_m=45Ω despite an unloaded quality factor (Q_{UL}) of 122

KEYWORDS

Flexure, coupling, PZT, resonator, MEMS

BACKGROUND

Military communications systems, such as SINCGARS, continue to rely on sub-100 MHz filters, and require frequency-agile filters with narrow bandwidth, exceptional stop-band rejection, and frequency trimming capabilities [1]. Thin-film PZT MEMS resonators offer the ability to achieve such requirements at low frequencies with low R_m and IL in an area-efficient footprint due to its high electromechanical coupling factors, enabling efficient energy transduction [2].

Piezoelectric MEMS devices commonly utilize flexure modes in a variety of sensing, energy harvesting, and actuation applications [2-5]. Despite a focus on flexure modes in the early RF MEMS literature [6], the advent of higher performance and higher frequency devices utilizing contour extensional modes [7] has led to few publications on their use in piezoelectric RF resonators over the past decade. Much of the early work on piezoelectric flexure mode RF resonators was based on traditional fundamental out-of-plane modes in clamped-clamped beams [8-10]. The use of non-traditional flexure modes has not been extensively explored for RF applications, particularly higher dimensional modes that possess more than one non-zero stress component [11].

High electromechanical coupling modes are of interest both as potential high performance resonators and as potential sources of spurious modes in filter applications. An improved understanding of electromechanical coupling and the behavior of the various families of normal modes of vibration can enable improved RF MEMS resonator and filter designs. The efficiency of energy transduction in piezoelectric devices is dependent upon which of the many quasi-static material electromechanical coupling factors are utilized in a particular resonator [12]. This is partly determined by which stress components are non-zero. Improved electromechanical coupling is generally achieved when more than one stress component contributes to energy transduction via an associated non-zero piezoelectric coefficient. This paper reports a low-loss and high-coupling device that illustrates the potential of utilizing non-traditional flexural modes, modes that exploit stronger electromechanical coupling due to higher dimensional mode shapes, and describes the associated family of normal modes.

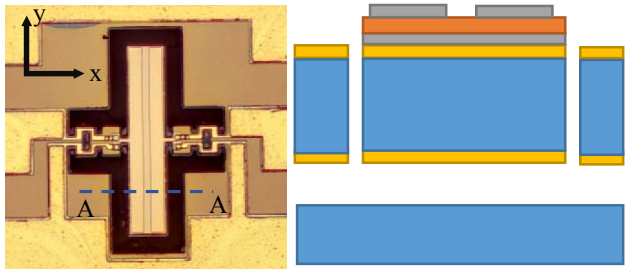

(a) (b)

Figure 1: (a) Micrograph of the 40 x 200 µm² PZT-silicon resonator (b) Illustration of cross section A-A. Device layers starting from bottom are: silicon handle wafer (blue), 0.1 µm buried oxide (yellow), 4 µm device silicon (blue), 0.2 µm top oxide (yellow), 0.12 µm bottom platinum (gray), 0.5 µm PZT (orange), and 0.1 µm top platinum

DESIGN AND MODELING

The motional resistance and figure of merit of a two-port resonator is inherently dependent on the degree of electromechanical coupling. On the input port, the modal force is dependent upon the overlap integral of the applied piezoelectric stress and the modal strain. On the output port, the current is dependent on the surface integral of the modal strain multiplied with the piezoelectric coefficient. In either case, the piezoelectric strain coefficient d matrix is a determining factor in which stresses and electric fields contribute to coupling. The mode explored in this work utilizes both the d_{31} and d_{32} coefficients, which are equal in PZT.

$$D_3 = \int_A (d_{31}\sigma_x + d_{32}\sigma_y) dA \qquad (1)$$

Equation (1) reveals that the use of vibrational modes that possess more than one non-zero, in phase normal-stress component will result in an enhancement of electric displacement and motional current. This is equally true for the generation of modal force and excitation of the mode. Equation (1) also highlights the relationship between piezoelectric electromechanical coupling and silicon thickness in out-of-plane flexure modes; the addition of silicon changes the stress state of the PZT, and hence electric displacement. In contrast to the commonly employed contour extensional modes, out-of-plane flexure modes in single-layer piezoelectric devices require additional non-piezoelectric material, such as silicon, to enhance coupling. The excitation of these modes requires bending stresses that can only be generated with structures that are asymmetric about either the x-z or x-y neutral planes. The stress components in Eq. (1) are functions of silicon thickness for out-of-plane flexure and are equal to zero for zero silicon thickness.

Figure 1a shows a micrograph, and Figure 1b a cross section of 200x40 μm^2 0.5-µm PZT on 4-µm silicon two-port resonator fabricated in the process described in [2]. In addition to enhancing coupling for out-of-plane flexure, the PZT-silicon stack offers trades between the high coupling of PZT and high mechanical Q of silicon, while enhancing power handling/linearity and maintaining near constant figures of merit, k_{eff}^2 Q, across PZT/silicon ratios for commonly employed contour extensional modes [13].

Simulation

The resonant mode explored in this work is associated with width flexure and features significant stresses in both the x and y dimensions. Displacement results from COMSOL modal analysis simulations of the fabricated device are show in Figure 2a, and Figure 2b shows the corresponding untethered mode. Comparison of figures reveals suppression of resonator displacement near tether locations.

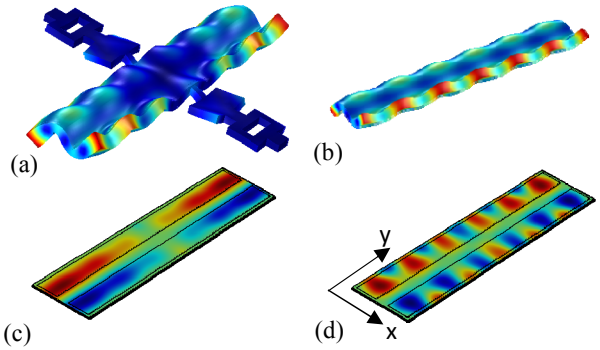

Figure 2: (a) Displacement results from COMSOL simulation of the fabricated device at 51.5 MHz (b) The corresponding mode in a device without tethers at 51.4 MHz (c) Modal x normal stress in PZT layer (d) Modal y normal stress in PZT layer. Flexure is excited due to the location of the piezoelectric layer off of the neutral axis. The similarity in the locations of the stresses and their phase results in enhanced coupling.

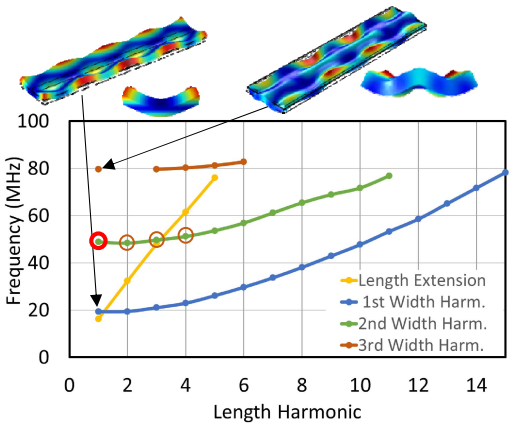

Figure 3: Frequency scaling of the family of normal modes with harmonics in length and width in an untethered device. The simulated devices shown in the figure depict the displacements of fundamental length mode of the 1st and 3rd width modes. Note the x-z profile resemblance to free-free beam flexure. For the device examined in the paper and its *fundamental mode, see Figure 2 and the point circled in red. Modes circles in brown correspond to the modes in Figure 4b,c,d. The yellow curve corresponding to length extension modes is included to illustrate the mode scaling with frequency.*

The x-z profiles of the deformed mode shapes, illustrated in Figure 3, clearly resemble the lower harmonics of a free-free beam in flexural vibration. The position of the PZT layer off of the x-z and y-z neutral planes allows out-of-plane flexural modes to be excited. If the PZT mid-plane coincided with these neutral planes, there would be no flexural excitation. Excitation may be taken to mean the overlap integral of the piezoelectrically generated stress and the modal strain has a non-zero value. The larger the value of this overlap integral, the more strongly a particular mode

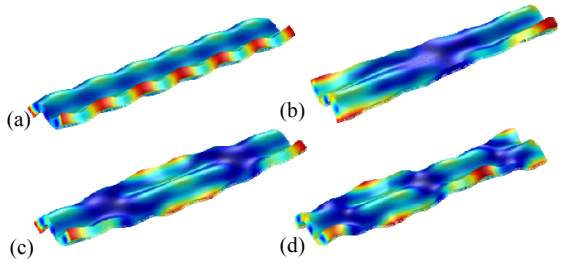

Figure 4: Displacement results from a COMSOL simulation of a free beam, with normal modes belonging to the 2nd width flexure family of Figure 3, the device family used in this paper. These displacement results show the (a) 1st, (b) 2nd, (c) 3rd, and (d) 4th harmonics in length. The mode investigated in this paper is (a). Nodal lines in the width demarcate a new length harmonic, and a 180° phase shift in z displacement

is excited. A mode with more than one relevant stress component has the potential to transduce more energy, given correct electrode design and crystal orientation to make use of coupling coefficients.

Figure 2c,d show the x and y modal stresses, respectively, in the piezoelectric layer for the mode in Figure 2a. It is apparent from Figures 2c,d that the modal stresses are in phase, and since d_{31} and d_{32} are of the same sign, electromechanical coupling is enhanced. Integration of the in-plane normal stresses over the electroded surfaces of the PZT in COMSOL confirms that the total force contribution in y from d_{32} is approximately 33% of the stress in x from d_{31}. This is in contrast to one-dimensional beam-like geometries, such as length extension and fundamental free-free flexure, which only utilize the d_{31} piezoelectric coefficient for coupling. Notably the stresses on the input and output port are of opposite sign, thus phase inversion occurs, unlike conventional length extension resonators.

Normal Mode Family Description

Figure 3 plots the resonant frequency versus harmonic number of the class of normal modes related to the mode investigated in this work. Extensional modes are plotted for reference. The comparison with the extensional modes highlights the nonlinear relationship between the length harmonic number and resonant frequency, and that these harmonics appear much closer together in frequency. This suggests spurious modes are likely to appear near the mode of interest, a non-trivial issue for the requirements of modern filters. Such modes are characterized by the presence of displacement nodal lines spanning length and width. Nodal lines spanning length correspond to harmonics

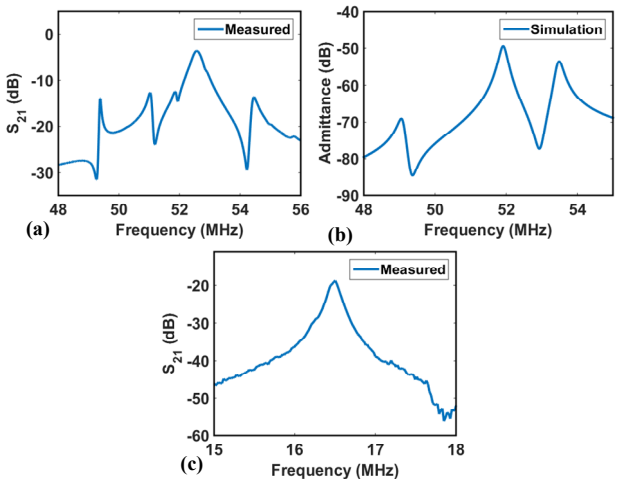

Figure 5: (a) Measured S_{21} data shows resonance at approximately 52.6 MHz with Q_{UL} of 122, k_{eff}^2 of 2.07%, and R_m of 44.9 (b) Admittance data from COMSOL frequency sweep simulation with resonance located at 51.9 MHz. (c) Measured S_{21} data of the length extension mode with resonance at 16.6 MHz, Q_{UL} of 118, k_{eff}^2 of 0.55%, and R_m of 749.

in the width flexure profile. Nodal lines spanning width demarcate a 180º phase shift in z-displacement, and harmonics in the length. To further illustrate the behavior of this family of modes, Figure 4a plots the displacement of the 2nd width, 1st length mode (the mode investigated), and its (b) 2nd, (c) 3rd, and (d) 4th length harmonics. These correspond to the modes highlighted in brown in Figure 3.

Dimensional Effect on Frequency

It is important to understand how the mode of interest behaves at higher frequencies and its dependence on device dimensions. The frequency of this mode is largely determined by the width dimension. For a set width, a varied length had a small effect on the frequency of the lowest harmonic, (under 1 MHz for L/W from 2:1 to 100:1). The mode is somewhat sensitive to changes in thickness. See Figure 3 for displacement simulations of the fundamental length harmonic in the 1st and 3rd width harmonics.

EXPERIMENTAL RESULTS

The scattering parameters were measured on a Rohde & Schwarz ZVB 8 network analyzer with a 10-V DC bias superimposed on both ports with a 50 Ω termination. Figure 5a shows the measured S-parameters of the mode of interest with -3.6 dB IL, k_{eff}^2=2.07, R_m=44.9Ω at 52.6 MHz with a Q_{UL} of 122, while Figure 5b shows extracted admittance data from COMSOL. This starkly contrasts the performance measured with the same device's fundamental length extension mode (Figure 5c) at 16.6 MHz (IL=-18.8 dB, Q_{UL}=118, k_{eff}^2=0.55%, R_m=749), a mode typically presented in MEMS publications. The nearly 4X improvement in k_{eff}^2 is attributed to the improved electromechanical coupling of the higher dimensional flexure mode shape and the influence of the silicon thickness that reduces coupling of the extensional mode while enhancing the coupling of the flexure mode. It should be noted that in the measured data of Figure 5a, the spur at approximately 55 MHz is believed to be the 2nd length, 2nd width harmonic (Figure 4b), closely related to the mode presented here. This illustrates the problem of the harmonic scaling with frequency, as the next harmonic is only a few MHz away. In filter applications, this would inhibit performance.

CONCLUSION AND FUTURE WORK

The demonstration of this compact, low R_m, high k_{eff}^2 device highlights the potential of utilizing non-traditional flexural modes and modes that exploit stronger electromechanical coupling due to higher dimensional mode shapes.

In contrast to length extension, coupling may be increased by adding material; when the silicon device layer thickness is zero, the mode should not be excited. Future work will quantify relationship between electromechanical coupling and silicon thickness in the modes reported here. Out-of-plane flexure may not outperform length extension in coupling for all thicknesses of the non-piezoelectric layer,

but there may exist a critical thickness where excellent power handling and linearity are traded for any losses in coupling.

Challenges facing this particular mode family for use in filters are the spurious response due to nearby harmonics and tethering resonators appropriately along the nodal points that exist along the shorter edges of the plate. This second point would likely increase the overlap integral, as stress in the width is directly related to curvature, which is suppressed by the current tether location.

ACKNOWLEDGEMENTS

This research was supported in part by an appointment to the Student Research Participation Program at the U.S. Army Research Laboratory (ARL), administered by the Oak Ridge Institute for Science and Education through an interagency agreement between the U.S. Department of Energy and US ARL. The authors would also like to thank Dr. Luz Sanchez, Joel Martin, and Brian Power for their efforts in fabrication.

REFERENCES

[1] M. McCorquodale, A. Wong, K. Nagarajan, H. Kulah, and C. Nguyen. "An Integrated MEMS-BiCMOS SINCGARS Transceiver", Design Automation Conference, (2000).

[2] J. S. Pulskamp, R. G. Polcawich, R. Q. Rudy, S. S. Bedair, R. M. Proie, T. Ivanov, and G. L. Smith, "Piezoelectric PZT MEMS technologies for small-scale robotics and RF applications," *MRS Bull.*, vol. 37, no. 11, pp. 1062–1070, Nov. 2012.

[3] P. Muralt, et al. "Piezoelectric micromachined ultrasonic transducers based on PZT thin films." *Ultrasonics, Ferroelectrics, and Frequency Control, IEEE Transactions on* 52.12 (2005): 2276-2288.

[4] Y.B. Jeon, et al. "MEMS power generator with transverse mode thin film PZT." *Sensors and Actuators A: Physical* 122.1 (2005): 16-22.

[5] S.C. Ko, et al. "Micromachined piezoelectric membrane acoustic device." *Sensors and Actuators A: Physical* 103.1 (2003): 130-134.

[6] Yao, J. Jason. "RF MEMS from a device perspective." Journal of Micromechanics and Microengineering 10.4 (2000): R9.

[7] G. Piazza, P. Stephanou, and A. Pisano. "Single-chip multiple-frequency ALN MEMS filters based on contour-mode piezoelectric resonators." *Microelectromechanical Systems, Journal of* 16.2 (2007): 319-328.

[8] G. Piazza, R. Abdolvand, and F. Ayazi. "Voltage-tunable piezoelectrically-transduced single-crystal silicon resonators on SOI substrate." *Micro Electro Mechanical Systems, 2003. MEMS-03 Kyoto. IEEE The Sixteenth Annual International Conference on*. IEEE, 2003.

[9] B. Piekarski, D. DeVoe, M. Dubey, R. Kaul, J.Conrad, R. Zeto, "Surface Micromachined Piezoelectric Resonant Beam Filters", Sensors and Actuators, A 91, 2001, pp.313-320.

[10] D.L. DeVoe, "Piezoelectric thin film micromechanical beam resonators', Sensors and Actutators, A 88, 2001, pp 263-272.

[11] J. Pulskamp, S. Bedair, R. Polcawich, G. Smith, J. Martin, B. Power, and S. Bhave. "Electrode-Shaping for the Excitation and Detection of Permitted Arbitrary Modes in Arbitrary Geometries in Piezoelectric Resonators", IEEE Transactions on Ultrasonic, Ferroelectrics, and Frequency Control, 59, 1043, (2012).

[12] *IEEE Standard on Piezoelectricity*, ANSI/IEEE Std. 176-1987, 1988.

[13] S.S. Bedair, et al. "Low loss micromachined lead zirconate titanate, contour mode resonator with 50Ω termination." *Micro Electro Mechanical Systems (MEMS), 2012 IEEE 25th International Conference on*. IEEE, 2012.

CONTACT

*J.M. Puder, tel: +1-301-394-0257;
jmp378@cornell.edu